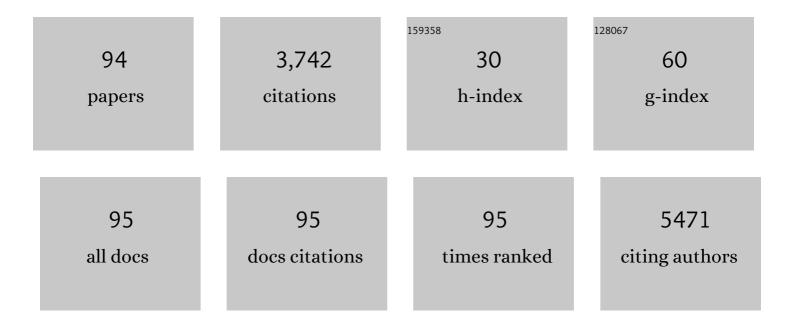
## De-Quan Yang

List of Publications by Year in descending order

Source: https://exaly.com/author-pdf/2265418/publications.pdf Version: 2024-02-01



#	Article	IF	CITATIONS
1	Ag NP catalysis of Cu ions in the preparation of AgCu NPs and the mechanism of their enhanced antibacterial efficacy. Colloids and Surfaces A: Physicochemical and Engineering Aspects, 2022, 632, 127831.	2.3	21
2	Leachability and Anti-Mold Efficiency of Nanosilver on Poplar Wood Surface. Polymers, 2022, 14, 884.	2.0	9
3	AFM/XPS Analysis of the Growth and Architecture of Oriented Molecular Monolayer by Spin Cast Process and Its Cross-Linking Induced by Hyperthermal Hydrogen. Applied Sciences (Switzerland), 2022, 12, 6233.	1.3	2
4	Dynamic behaviours and drying processes of water droplets impacting on superhydrophilic surfaces. Surface Engineering, 2021, 37, 1301-1307.	1.1	3
5	A facile route to prepare colorless Ag-Cu nanoparticle dispersions with elevated antibacterial effects. Colloids and Surfaces A: Physicochemical and Engineering Aspects, 2021, 626, 127116.	2.3	9
6	Destabilization of PVA-stabilized Ag NPs: color changes at low aqueous concentrations, induced by aggregation and coalescence. Materials Research Express, 2020, , .	0.8	5
7	Synthesis of amorphous SiO <sub>2</sub> nanowires by one-step low temperature hydrothermal process. Materials Research Express, 2019, 6, 115202.	0.8	3
8	A facile method to prepare mechanically durable super slippery polytetrafluoroethylene coatings. Colloids and Surfaces A: Physicochemical and Engineering Aspects, 2018, 556, 99-105.	2.3	28
9	Improving the Mechanical Durability of Superhydrophobic Coating by Deposition onto a Mesh Structure. Materials Research Express, 2018, 5, 065521.	0.8	4
10	Improved adhesion of Ag NPs to the polyethylene terephthalate surface via atmospheric plasma treatment and surface functionalization. Applied Surface Science, 2017, 411, 411-418.	3.1	38
11	Preparation of largeâ€scale, durable, superhydrophobic PTFE films using rough glass templates. Surface and Interface Analysis, 2017, 49, 1422-1430.	0.8	14
12	A study of the mechanical and chemical durability of Ultra-Ever Dry Superhydrophobic coating on low carbon steel surface. Colloids and Surfaces A: Physicochemical and Engineering Aspects, 2016, 497, 16-27.	2.3	34
13	An environment-friendly fabrication of superhydrophobic surfaces on steel and magnesium alloy. Materials Letters, 2016, 171, 297-299.	1.3	37
14	Preparation of anti-reflection glass surface with self-cleaning and anti-dust by ammonium hydroxide hydrothermal method. Materials Express, 2015, 5, 280-290.	0.2	11
15	Large-scale synthesis of 3D sphere-like hierarchical Ni(OH)2 nanofibers for high-performance electrochemical supercapacitors. Materials Research Express, 2015, 2, 095008.	0.8	3
16	Repelling hot water from superhydrophobic surfaces based on carbon nanotubes. Journal of Materials Chemistry A, 2015, 3, 16953-16960.	5.2	70
17	Aqueous synthesis and growth of morphologically controllable, hierarchical Ni(OH)2 nanostructures. Materials Research Express, 2015, 2, 075011.	0.8	3
18	Durable superhydrophobic PTFE films through the introduction of micro- and nanostructured pores. Applied Surface Science, 2015, 339, 151-157.	3.1	60

#	Article	IF	CITATIONS
19	How to repel hot water from a superhydrophobic surface?. Journal of Materials Chemistry A, 2014, 2, 10639-10646.	5.2	62
20	A New Approach of Tailoring Wetting Properties of TiO <sub>2</sub> Nanotubular Surfaces. Advanced Science Letters, 2012, 18, 158-163.	0.2	0
21	An Innovative Approach to Synthesize Highly-Ordered TiO <sub>2</sub> Nanotubes. Journal of Nanoscience and Nanotechnology, 2011, 11, 1079-1083.	0.9	3
22	Study of a hydrogen-bombardment process for molecular cross-linking within thin films. Journal of Chemical Physics, 2011, 134, 074704.	1.2	11
23	Stabilization of platinum nanoparticles on graphene by non-invasive functionalization. Carbon, 2009, 47, 2233-2238.	5.4	16
24	The unexpected formation of Aul̃′+–Sil̃′â~' by the resonance neutralization of Ar+ during the low energy bombardment of Au nanoparticles on c-Si. Applied Surface Science, 2009, 255, 6870-6874.	3.1	0
25	Characterization and Oxidation of Fe Nanoparticles Deposited onto Highly Oriented Pyrolytic Graphite, Using X-ray Photoelectron Spectroscopy. Journal of Physical Chemistry C, 2009, 113, 6418-6425.	1.5	37
26	Template―and Surfactantâ€free Room Temperature Synthesis of Selfâ€Assembled 3D Pt Nanoflowers from Singleâ€Crystal Nanowires. Advanced Materials, 2008, 20, 571-574.	11.1	232
27	The surface analytical characterization of carbon fibers functionalized by H2SO4/HNO3 treatment. Carbon, 2008, 46, 196-205.	5.4	494
28	Formation of a Porous Platinum Nanoparticle Froth for Electrochemical Applications, Produced without Templates, Surfactants, or Stabilizers. Chemistry of Materials, 2008, 20, 4677-4681.	3.2	27
29	A Facile Route for the Self-Organized High-Density Decoration of Pt Nanoparticles on Carbon Nanotubes. Journal of Physical Chemistry C, 2008, 112, 11717-11721.	1.5	46
30	Strongly Enhanced Interaction between Evaporated Pt Nanoparticles and Functionalized Multiwalled Carbon Nanotubes via Plasma Surface Modifications:  Effects of Physical and Chemical Defects. Journal of Physical Chemistry C, 2008, 112, 4075-4082.	1.5	79
31	Synthesis and Characterization of Platinum Nanowire–Carbon Nanotube Heterostructures. Chemistry of Materials, 2007, 19, 6376-6378.	3.2	100
32	Structure and Morphology of Co Nanoparticles Deposited onto Highly Oriented Pyrolytic Graphite. Journal of Physical Chemistry C, 2007, 111, 17200-17205.	1.5	25
33	X-ray Photoelectron Spectroscopic Analysis of Pt Nanoparticles on Highly Oriented Pyrolytic Graphite, Using Symmetric Component Line Shapes. Journal of Physical Chemistry C, 2007, 111, 565-570.	1.5	90
34	Core/Shell Formation of Gold Nanoparticles Induced on Exposure toN,N-Dimethylformamide:  Chemical and Morphological Changes. Journal of Physical Chemistry C, 2007, 111, 14320-14326.	1.5	1
35	Accurate Assembly and Size Control of Cu Nanoparticles into Nanowires by Contact Atomic Force Microscope-Based Nanopositioning. Journal of Physical Chemistry C, 2007, 111, 10105-10109.	1.5	5
36	Carbon 1s X-ray Photoemission Line Shape Analysis of Highly Oriented Pyrolytic Graphite:  The Influence of Structural Damage on Peak Asymmetry. Langmuir, 2006, 22, 860-862.	1.6	145

#	Article	IF	CITATIONS
37	XPS Demonstration of ï€â~ï€ Interaction between Benzyl Mercaptan and Multiwalled Carbon Nanotubes and Their Use in the Adhesion of Pt Nanoparticles. Chemistry of Materials, 2006, 18, 5033-5038.	3.2	138
38	Room temperature air oxidation of nanostructured Si thin films with varying porosities as studied by x-ray photoelectron spectroscopy. Journal of Applied Physics, 2006, 99, 084315.	1.1	4
39	Evidence of the Interaction of Evaporated Pt Nanoparticles with Variously Treated Surfaces of Highly Oriented Pyrolytic Graphite. Journal of Physical Chemistry B, 2006, 110, 8348-8356.	1.2	55
40	Platinum Nanoparticle Interaction with Chemically Modified Highly Oriented Pyrolytic Graphite Surfaces. Chemistry of Materials, 2006, 18, 1811-1816.	3.2	42
41	Electrophoretic separation of aniline derivatives using fused silica capillaries coated with acid treated single-walled carbon nanotubes. Journal of Chromatography A, 2005, 1074, 187-194.	1.8	70
42	Microscale chemical and electrostatic surface patterning of Dow Cyclotene by N2 plasma. Applied Surface Science, 2005, 242, 419-427.	3.1	1
43	The surface modification of nanoporous SiOx thin films with a monofunctional organosilane. Applied Surface Science, 2005, 252, 1197-1201.	3.1	13
44	The creation of Au nanoscale surface patterns by the low energy Ar + beam irradiation of Au clusters evaporated onto a SiO2/Si surface. Applied Physics A: Materials Science and Processing, 2005, 80, 575-579.	1.1	4
45	Photoluminescence of highly porous nanostructured Si-based thin films deposited by pulsed laser ablation. Journal of Applied Physics, 2005, 98, 024310.	1.1	10
46	Photoacoustic Fourier transform infrared spectroscopy of nanoporous SiOxâ^•Si thin films with varying porosities. Journal of Applied Physics, 2005, 98, 114310.	1.1	12
47	Room temperature oxidation kinetics of Si nanoparticles in air, determined by x-ray photoelectron spectroscopy. Journal of Applied Physics, 2005, 97, 024303.	1.1	87
48	Controlled Chemical Functionalization of Multiwalled Carbon Nanotubes by Kiloelectronvolt Argon Ion Treatment and Air Exposure. Langmuir, 2005, 21, 8539-8545.	1.6	70
49	Oxidation, Deformation, and Destruction of Carbon Nanotubes in Aqueous Ceric Sulfate. Journal of Physical Chemistry B, 2005, 109, 1400-1407.	1.2	38
50	Functionalization of Multiwalled Carbon Nanotubes by Mild Aqueous Sonication. Journal of Physical Chemistry B, 2005, 109, 7788-7794.	1.2	129
51	Spectroscopic Evidence for Ï€â^'Ï€ Interaction between Poly(diallyl dimethylammonium) Chloride and Multiwalled Carbon Nanotubes. Journal of Physical Chemistry B, 2005, 109, 4481-4484.	1.2	265
52	Surface Diffusion and Coalescence of Mobile Metal Nanoparticles. Journal of Physical Chemistry B, 2005, 109, 9703-9711.	1.2	343
53	Interaction of Evaporated Nickel Nanoparticles with Highly Oriented Pyrolytic Graphite:Â Back-bonding to Surface Defects, as Studied by X-ray Photoelectron Spectroscopy. Journal of Physical Chemistry B, 2005, 109, 19329-19334.	1.2	37
54	Excimer laser manipulation and pattering of gold nanoparticles on the SiO2/Si surface. Journal of Applied Physics, 2004, 95, 5023-5026.	1.1	23

#	Article	IF	CITATIONS
55	Optical breakdown processing: Influence of the ambient gas on the properties of the nanostructured Si-based layers formed. Journal of Applied Physics, 2004, 95, 5722-5728.	1.1	14
56	The early stages of silicon surface damage induced by pulsed CO2 laser radiation: an AFM study. Applied Surface Science, 2004, 222, 365-373.	3.1	8
57	Formation of densely populated SiOx microtree-like structures on the Si (100) surface using excimer laser irradiation in air. , 2004, 5578, 652.		3
58	A spectroscopic study of CNx formation by the keV N2+ irradiation of highly oriented pyrolytic graphite surfaces. Surface Science, 2003, 531, 185-198.	0.8	19
59	The manipulation of Cu cluster dimensions on highly oriented pyrolytic graphite surfaces by low energy ion beam irradiation. Surface Science, 2003, 536, 67-74.	0.8	11
60	The applicability of angle-resolved XPS to the characterization of clusters on surfaces. Surface Science, 2003, 536, 139-144.	0.8	22
61	Cu cluster adhesion enhancement on the modified Dow Cyclotene surface through low energy N2+ beam irradiation at grazing angles. Applied Surface Science, 2003, 207, 1-5.	3.1	8
62	Local surface cleaning and cluster assembly using contact mode atomic force microscopy. Applied Surface Science, 2003, 210, 158-164.	3.1	9
63	Porous nanostructured layers on germanium produced by laser optical breakdown processing. , 2003, , .		1
64	The quantitative correlation of nanoscopic and macroscopic measurements of adhesion: copper clusters on a low-permittivity polymer. Journal of Physics Condensed Matter, 2002, 14, 7097-7100.	0.7	7
65	s–p Hybridization in highly oriented pyrolytic graphite and its change on surface modification, as studied by X-ray photoelectron and Raman spectroscopies. Surface Science, 2002, 504, 125-137.	0.8	111
66	The surface modification of Dow Cyclotene by low energy N2+ beams and its effect on the adhesion of evaporated Cu films. Applied Surface Science, 2002, 195, 202-213.	3.1	4
67	Ar+-induced surface defects on HOPG and their effect on the nucleation, coalescence and growth of evaporated copper. Surface Science, 2002, 516, 43-55.	0.8	61
68	Initial- and final-state effects on metal cluster/substrate interactions, as determined by XPS: copper clusters on Dow Cyclotene and highly oriented pyrolytic graphite. Applied Surface Science, 2002, 195, 187-195.	3.1	60
69	Coalescence kinetics of copper clusters on highly oriented pyrolytic graphite and Dow Cyclotene, as determined by x-ray photoelectron spectroscopy. Journal of Applied Physics, 2001, 90, 4768-4771.	1.1	25
70	Interface configuration and metal adhesion in Au-polycarbonate bilayer structure: Influence of 27Al+ ion mixing. Journal of Vacuum Science and Technology A: Vacuum, Surfaces and Films, 2001, 19, 848-855.	0.9	1
71	The estimation of the average dimensions of deposited clusters from XPS emission intensity ratios. Applied Surface Science, 2001, 173, 134-139.	3.1	39
72	Nitrogen plasma treatment of the dow Cyclotene 3022 surface and its reaction with evaporated copper. Applied Surface Science, 2001, 177, 85-95.	3.1	31

#	Article	IF	CITATIONS
73	The enhancement of the adhesion of copper layers to Dow Cyclotene 3022 through metal sputtering. Applied Surface Science, 2001, 180, 200-208.	3.1	12
74	Electrical properties of bis(4-diethyannodithiobenzil)nickel and stearyl alcohol mixed Langmuir–Blodgett films. Thin Solid Films, 2001, 385, 239-245.	0.8	1
75	Sizes correction on AFM images of nanometer spherical particles. Journal of Materials Science, 2001, 36, 263-267.	1.7	30
76	Argon ion treatment of the Dow Cyclotene 3022 surface and its effect on the adhesion of evaporated copper. Applied Surface Science, 2001, 173, 30-39.	3.1	21
77	Preparation and characterization of nanostructured silver thin films deposited by radio frequency magnetron sputtering. Thin Solid Films, 2000, 375, 300-303.	0.8	33
78	The surface structure of Dow Cyclotene 3022, as determined by photoacoustic FTIR, confocal Raman and photoelectron spectroscopies. Applied Surface Science, 2000, 165, 15-22.	3.1	22
79	Interfacial reaction between evaporated copper and Dow Cyclotene 3022. Applied Surface Science, 2000, 165, 116-126.	3.1	24
80	Study on nucleation and growth of Ag nanoparticles prepared by radio-frequency sputtering on highly oriented pyrolytic graphite and amorphous carbon. Journal of Vacuum Science & Technology an Official Journal of the American Vacuum Society B, Microelectronics Processing and Phenomena, 2000, 18, 1156.	1.6	4
81	Attenuation Lengths of Photoelectrons in BDN-SA Langmuir-Blodgett Films. Molecular Crystals and Liquid Crystals, 1999, 337, 65-68.	0.3	1
82	Structural studies of functional organized molecular thin films using angle-resolved X-ray photoelectron spectroscopy. Applied Surface Science, 1999, 144-145, 451-455.	3.1	6
83	Preparation and structural characterization of nanostructured iron oxide thin films. Applied Surface Science, 1999, 147, 39-43.	3.1	23
84	X-ray photoelectron spectroscopy of nickel dithiolene complex Langmuir–Blodgett films. Applied Surface Science, 1999, 148, 196-204.	3.1	8
85	Title is missing!. Journal of Materials Science, 1999, 34, 5569-5574.	1.7	1
86	Preparation and conductivity of dithiolene complex Langmuir–Blodgett films. Journal of Materials Science: Materials in Electronics, 1999, 10, 557-561.	1.1	0
87	Unlubricated friction and wear behaviour of zirconia ceramics. Wear, 1998, 215, 232-236.	1.5	29
88	Study of the environment effect on the properties of BDN-SA Langmuir–Blodgett films. Thin Solid Films, 1998, 320, 316-319.	0.8	6
89	Microcrystalline domains of monolayer and multilayer BDN-SA Langmuir–Blodgett films. Supramolecular Science, 1998, 5, 615-617.	0.7	0
90	Dependence of Secondary Ion Mass Spectrometry Relative Sensitivity Factor on Matrix. Chinese Physics Letters, 1998, 15, 697-699.	1.3	3

#	Article	IF	CITATIONS
91	<title>N2H4 gas detection using Langmuir-Blodgett films of a dithiolene complex on chemiresistor sensors</title> . , 1998, 3175, 82.		3
92	Microcrystalline Domains of Monolayer and Multilayer Dithiolene Langmuir-Blodgett Films Studied by AFM. Physica Status Solidi (B): Basic Research, 1997, 203, R7-R8.	0.7	1
93	Voltammetric determination of hydrazine based on catalytic reaction in the presence of 4-hydroxy-2,2,6,6-tetramethyl-piperdinyloxy (TEMPOL) radical. Electroanalysis, 1997, 9, 1429-1431.	1.5	8
94	Changes in alloy surface composition induced by low energy ion bombardment. Vacuum, 1992, 43, 231-234.	1.6	4